*Inorg. Chem.* **2006**, *45*, 8175–8178


# $Mg_{5.23}Sm_{0.77}Sb_4$: an Ordered Superstructure Derived from the $Mg_3Sb_2$ Structure Type

**Shalabh Gupta,[†,‡] Ashok K. Ganguli,*[,†,‡] and John D. Corbett*[,†]**

*Department of Chemistry, Iowa State University, Ames, Iowa 50011, and Department of Chemistry, Indian Institute of Technology Delhi, Hauz Khas, New Delhi 110016, India*

Received May 15, 2006

The ternary polar intermetallic phase $Mg_{5.231(8)}Sm_{0.769(8)}Sb_4$ has been obtained from solid-state reactions at 700–850 °C in sealed Ta or Nb containers when the synthetic conditions took into account its characteristic incongruent melting point. The compound crystallizes in the trigonal space group $P\bar{3}$ ($Z = 1$) with $a = 4.618(1)$ Å and $c = 14.902(6)$ Å in a structure that derives from that of $Mg_3Sb_2$ (anti-$La_2O_3$ type). This composition appears to be near the lower limit of Sm content, and solutions with appreciably higher Sm contents are also stable [$Mg_{6-x}Sm_xSb_4$, $x \leq 1$]. The result provides the first example of a superstructure of a $Mg_3Sb_2$-like structure with a doubled $c$ axis induced by ordering a mixture of the larger divalent Sm and Mg ions separately within alternate layers of octahedral sites. Still larger proportions of Sm also give rise to a second solid solution region in the parent $Mg_3Sb_2$ type structure ($P\bar{3}m1$), $Mg_{3-y}Sm_ySb_4$, $0 \leq y \leq 1$. Retention of the same $3e^-$ valence electron counts per antimony in all of these phases suggests that the compounds remain electron precise and Zintl phases. Analogous compounds with Ca, Sr, or Ba substitution have evidently not been investigated.

## 1. Introduction

Significant research activity continues in the broad area of polar intermetallics because interesting and hitherto unknown structure types with novel bonding patterns are quite often encountered.[1−3] Another pressing reason for activity in this area, which remains highly exploratory in nature, is because of the interesting electronic properties of some examples. Of special interest to various investigators are the stannides and antimonides as some exhibit promising thermoelectric[4,5] and magnetic properties.[6] Typical polar intermetallics are formed between electropositive elements (alkali or alkaline-earth metals) and the elements around the Zintl border (groups 13−15). These may exhibit a rich variety of structural features that require understanding of new concepts, such as metallic Zintl phases[7,8] and the diverse effects of packing and nonclassical bonding.[9−11] It has been noted in the literature[12] that the structure and stabilities of the ionic cluster salts may be influenced to a major degree by packing, electronic effects, and Madelung energies. In this regard, mixed cations have often been found to be instrumental in stabilizing a diverse variety of anionic cluster species in new and unusual structures in closely related systems.[1]

In this report, we describe a new mixed cation superstructure derived from $Mg_3Sb_2$ by ordered substitution of up to one-half of the octahedrally coordinated Mg by dipositive Sm. Ternary compounds with a $Mg_3Sb_2$ structure type are known mainly with substitutions in all of the octahedra metal layers, such as in $AeMg_2Sb_2$ in which Ae is Ca, Sr, or Ba.[13] Potential derivatives with trivalent rare-earth elements would of course require other substitutions as well in order to retain closed-shell stability, as found in the $CaAl_2Tt_2$ analogues for

* To whom correspondence should be addressed. Email: jcorbett@iastate.edu (J.D.C.); ashok@chemistry.iitd.ernet.in (A.K.G.).
† Iowa State University.
‡ Indian Institute of Technology Delhi.

(1) Corbett, J. D. *Angew. Chem., Int. Ed.* **2000**, *39*, 670.
(2) Corbett, J. D. In *Chemistry, Structure and Bonding of Zintl Phases and Ions*; Kauzlarich, S., Ed., VCH: New York, 1996; Chapter 3.
(3) Schaefer, H. *Annu. Rev. Mater. Sci.* **1985**, *15*, 1.
(4) Gascoin, F.; Ottensmann, S.; Stark, D.; Haile, S. M.; Snyder, G. J. *Adv. Funct. Mater.* **2005**, *15*, 1860.
(5) Dashjav, E.; Szczepenowska, A.; Kleinke, H. *J. Mater. Chem.* **2002**, *12*, 345.
(6) Crerar, S, J.; Deakin, L.; Mar, A. *Chem. Mater.* **2005**, *17*, 2780.
(7) Nesper, R. *Prog. Solid State Chem.* **1990**, *20*, 1.
(8) Nesper, R. *Angew Chem., Int. Ed. Engl.* **1991**, *30*, 789.
(9) Corbett, J. D. *Chem. Rev.* **1985**, *85*, 383.
(10) Sevov, S. C.; Corbett, J. D. *Inorg. Chem.* **1991**, *30*, 4875.
(11) Dong, Z.-C.; Corbett, J. D. *J. Am. Chem. Soc.* **1994**, *116*, 3429.
(12) Ganguli, A. K.; Corbett, J. D.; Köckerling, M. *J. Am. Chem. Soc.* **1998**, *120*, 1223.
(13) Deller, K.; Eisenmann, B. *Z. Naturforsch.* **1977**, *32B*, 612.

10.1021/ic060835w CCC: $33.50 
Published on Web 09/02/2006

Tt = Si, Ge.[14] Ternary antimonide examples with rare-earth elements that reinforced our interests in this area were the three intergrowth structures reported by Ganguli, et al.[15] in the Mg−La−Sb system. These novel Zintl phases can be described in terms of coherent intergrowths between either $Mg_5Sb_4$ or $Mg_2Sb_2$ units derived from the $Mg_3Sb_2$ structure and $La_{n+1}Sb_n$ slabs from LaSb (NaCl-type structure). The longer and hence presumably weaker Mg(oct)−Sb bonds at 3.11 Å in comparison with stronger Mg(tetrah)−Sb bonds that average 2.84 Å provide the required flexibility for the rare-earth element substitution at the former site. However, the observed (001)−(111) intergrowth was believed to be additionally constrained to LnSb phases that have $a/\sqrt{2}$ values comparable to the *a* dimension of $Mg_3Sb_2$ (4.56 Å). It was realized that further possibilities of deriving novel ternary phases in this kind of system were not exhausted, and this was the sole motivation behind the present work. One possibility would be to substitute tin for antimony to eliminate the cation defects, and another more obvious one would be similar intergrowths with other rare-earth metal antimonides. However, the latter proved unsuccessful for Ln = Pr, Nd, Gd, and Tb, only $Mg_3Sb_2$ and LnSb forming as major products. Lattice mismatch that induced strain was thought to preclude intergrowths with these other trivalent rare-earth element antimonides. On the other hand, attempted substitution of divalent example Sm did afford the new superstructure variation of $Mg_3Sb_2$ reported here.

## 2. Experimental Section

**2.1. Syntheses.** Single crystals of a $Mg_{5.231(8)}Sm_{0.769(8)}Sb_4$ (nominally 5−1−4) composition according to later single-crystal analysis were obtained after a mixture of the high-purity elements as Mg turnings (99.99%, Ames Laboratory), Sm powder (Research Chemicals, 99.9%), and Sb chunks (99.99%, Johnson−Matthey) was allowed to react at high temperature in Ta or Nb tubing (1/4 in. diam) welded under an Ar atmosphere. The tubes were further jacketed in evacuated and sealed silica containers and heated in resistance furnaces. The new phase was first recognized via high-quality Guinier patterns obtained with the aid of a Huber 670 Guinier powder camera equipped with an area detector. The 5−1−4 phase was present in only ca. 30% yield following a reaction of the nominal composition $Mg_{2.5}Sm_{0.5}Sb_2$ in Ta at 850 °C for 7 days followed by radiative cooling. However, four other phases were also present, $Mg_3Sb_2$ (∼15%), $Ta_5Sb_4$ (∼10%), SmSb (∼20%), and $Sm_{3-x}Mg_xSb_2$ (∼25%). The last, presumably with random substitution of Sm for Mg, was recognized (in several instances) from its $Mg_3Sb_2$-like powder pattern, mainly through an increase in *d* values of the reflections. This particular system was possibly not at equilibrium. (The $Ta_5Sb_4$ side product from attack of the Ta container was, as before in related systems,[16] avoided thereafter by the use of Nb.) An identical composition $Mg_{2.5}Sm_{0.5}Sb_2$ yielded ∼80% of the new (5−1−4) phase along with ∼20% SmSb when the elemental components were allowed to react at 700 °C for 10 days in a Nb container. On the other hand, the same reaction mixture quenched from 850 or 1000 °C followed by annealing at 400 or 600 °C yielded none of the new phase. Subsequently, a series of three stoichiometries, that of the crystal composition and two that were richer in Sm and poorer in Mg, were studied under three different reaction conditions in order to obtain the new phase more cleanly and in higher yields. Slow cooling from 850 °C yielded moderate amounts of the product, some with noticeably large cells. However, quenching of the samples from 950 °C followed by 10 day equilibrations at 700 °C gave the highest yields, in particular 85% 5−1−4 plus only SmSb from a $Mg_4Sm_2Sb_4$ composition, the latter suggesting that this loading was too rich in Sm. At the same time, the cell volumes were observed to increase appreciably, from 275.3 $Å^3$ for the structurally refined product through intermediate values above 290 $Å^3$ to the maximum seen for the last sample, 292.6 $Å^3$ ($a$ = 4.686 Å, $c$ = 15.388 Å). The new phase is not very sensitive to air at room temperature.

Substitution of Yb in the smaller parent structure was also observed with different stoichiometries. However, Lu instead in similar proportions and conditions did not lead to the superstructure phase. Instead, only $Mg_3Sb_2$ and LuSb were formed, which suggests that there are likely dipositive charge limitations to stabilizing substitutional products in this structure.

**2.2. Powder X-ray Diffraction.** The powder diffraction patterns of all products obtained with the aid of a Huber 670 camera and Cu Kα1 radiation were used for phase identification. Samples were mounted inside a nitrogen-filled glovebox between two Mylar sheets by means of a block-and-ring assembly and some vacuum grease to hold and to seal the sample from the air. The presence of the title and other phases were established by matching the observed patterns with those of known phases generated from their lattice parameters, space groups, and atomic positions, the last for the title phase according to the single-crystal analysis.

**2.3. Single-Crystal Structure Determination.** A few small black irregular crystals of the title compound were isolated from the products from the first reaction (with a loaded composition $Mg_{2.5}Sm_{0.5}Sb_2$) and placed inside glass capillaries (0.3 mm) under a nitrogen atmosphere. These were flame-sealed, and the crystals were checked for singularity. An irregularly shaped one with approximate dimensions of 0.08 mm × 0.07 mm × 0.07 mm was used for the X-ray crystallographic analysis at 293 (2) K. Data were collected on a Bruker SMART[17] APEX CCD system equipped with an area detector, a graphite monochromator, and a Mo Kα fine-focus sealed tube ($\lambda$ = 0.71073 Å). The detector was placed at a distance of 4.995 cm from the crystal. A total of 1800 frames were collected for the indicated trigonal cell with $\omega - 2\Theta$ scans, a scan width of 0.3°, and an exposure of 10 s/frame. The total data collection time was approximately 8 h. The frames were integrated by means of the Bruker SAINT software package[17] and the narrow-frame integration algorithm. The process yielded a total of 1865 reflections to a maximum $\theta$ angle of 28.20° (0.75 Å resolution), of which 433 were independent and observed [$I > 2\sigma(I)$] (completeness = 91.9%, $R_{int}$ = 10.44**%**). Analysis of the data showed negligible decay during the measurements. Data were corrected for absorption effects with the aid of the multiscan technique SADABS.[18] Some data collection and refinement parameters are tabulated in Table 1.

The structure was solved by direct methods and refined by least-squares methods on $F_0^2$ with the Bruker SHELXTL (Version 6.1) software package.[19] Space group $P\bar{3}$ (No. 147) was chosen on the basis of the lack of any systematic absences and the *E* value

(14) Gladyshevskii, E. J.; Kripyakevich, P. I.; Bodak, O. I. *Ukr. Phys. J.* **1967**, *12*, 447.
(15) Ganguli, A. K.; Kwon, Y, −U.; Corbett, J. D. *Inorg. Chem.* **1993**, *32*, 4354.
(16) Ganguli, A. K.; Gupta, S.; Corbett, J. D. *Inorg. Chem.*, **2006**, *45*, 196.
(17) *Bruker SMART and SAINT*; Bruker AXS Inc.: Madison, WI, 1998.
(18) Sheldrick, G. M. *SADABS user guide*; University of Göttingen: Göttingen, Germany, 1997.
(19) Sheldrick, G. M. *SHELXTL*, ver. 6.10; Bruker AXS, Inc.: Madison, WI, 2001.

**Table 1.** Some Crystal and Structure Refinement Data for $Mg_{5.231(8)}Sm_{0.769(8)}Sb_4$

| | |
|---|---|
| fw | 729.78 |
| crystal system | trigonal |
| space group, $Z$ | $P\bar{3}$ (No. 147), 1 |
| unit cell dimens (Å) | $a = 4.619(1)$ |
| | $c = 14.902(6)$ |
| vol (Å$^3$) | 275.3(1) |
| $d_{calc}$ (Mg/m$^3$) | 4.401 |
| $\mu$ (Mo K$\alpha$) (mm$^{-1}$) | 15.147 |
| data/restraints/params | 433/0/18 |
| final $R$ indices[a] [$I > 2\sigma(I)$[a]] | |
| R1, wR2 | 0.0480, 0.1028 |

[a] $R1 = \sum(|F_o| - |F_c|)/\sum(|F_0|)$, $wR2 = [\sum w(F_o^2 - F_c^2)/\sum wF_o^4]^{1/2}$

**Table 2.** Atomic Coordinates ($\times 10^4$) and Equivalent Isotropic Displacement Parameters ($\times 10^3$ Å$^2$) for $Mg_{5.231(8)}Sm_{0.769(8)}Sb_4$

| | Wykoff | $x$ | $y$ | $z$ | $U_{(eq)}$[a] | occupancy ≠ 1 |
|---|---|---|---|---|---|---|
| Sm/Mg1 | 1a | 0 | 0 | 0 | 14(1) | 0.769(8)/0.231 |
| Sb1 | 2d | 1/3 | 2/3 | 3889(1) | 19(1) | |
| Sb2 | 2d | 1/3 | 2/3 | 1301(1) | 19(1) | |
| Mg2 | 2d | 1/3 | 2/3 | 1927(6) | 24(2) | |
| Mg3 | 2d | 1/3 | 2/3 | 3264(5) | 24(2) | |
| Mg4 | 1b | 0 | 0 | 5000 | 40(3) | |

[a] $U_{(eq)}$ is defined as one-third of the trace of the orthogonalized $U_{ij}$ tensor.

**Table 3.** Important Interatomic Distances (Å)

| bond | | distance |
|---|---|---|
| Sm/Mg1−Sb2 | ×6 | 3.297(1) |
| Mg2−Sb1 | ×1 | 2.928(8) |
| Mg2−Sb2 | ×3 | 2.823(3) |
| Mg3−Sb1 | ×3 | 2.824(2) |
| Mg3−Sb2 | ×1 | 2.925(8) |
| Mg4−Sb1 | ×6 | 3.138(1) |

statistics. No inconsistent equivalents were observed for the chosen space group. The successful solution of the structure and its final refinement affirmed this selection. No satisfactory solution could be obtained in the higher symmetry space group $P\bar{3}m1$ to which $Mg_3Sb_2$ belongs. The initial model correctly revealed the positional coordinates for Sm and Sb, but three improbable Mg positions also so generated were deleted during the refinement. Rather, the Mg positions were determined from a difference Fourier map. Two of the most intense residual peaks generated after the first few cycles of refinement were assigned as Mg, and the model was refined for a few more cycles. At this stage, all the atoms were refined anisotropically which led to well-behaved ellipsoids for all atoms. However, high values of R1 and wR2 (10% and 16%, respectively) and large anisotropic displacement parameters for Sm suggested that this site might be either partially occupied or co-occupied by Mg. The latter was employed in the final model, as it provided a slightly better fit over the former; furthermore, vacancies on this dipositive cation site would not be reasonable either considering the Sb proportion. The final anisotropic full-matrix least-squares refinement on $F_o^2$ with 18 variables converged at R1 = 4.8% for the 433 observed data and wR2 = 10.66% for all data. The final positional parameters and isotropic-equivalent displacement parameters for all atoms are collected in Table 2. More complete data are given in Supporting Information.

## 3. Results and Discussion

Intergrowth structures of $Mg_3Sb_2$ with rock-salt layers of LaSb that were demonstrated in our earlier report for three classic examples in the ternary Mg−La−Sb intermetallic

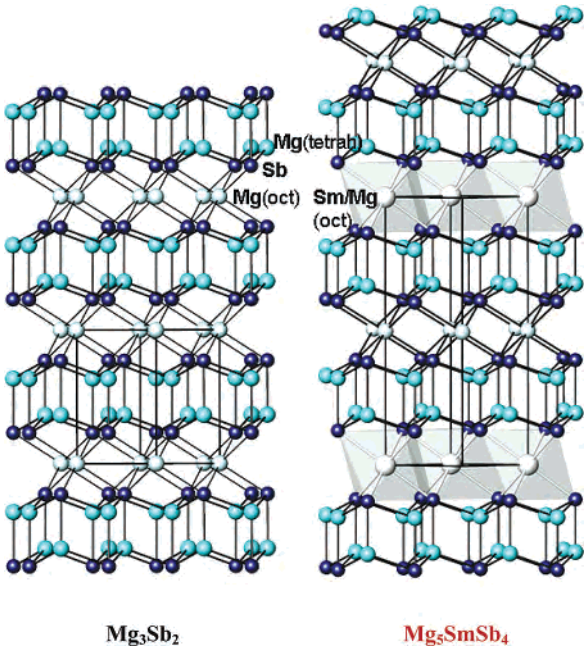


**Figure 1.** ~[110] projections of portions of the parent structure $Mg_3Sb_2$ (left) and of the superstructure $Mg_5SmSb_4$ (limiting composition) (right). Atom positions are marked as dark blue, Sb; medium blue, Mg in tetrahedral sites; light blue, Mg in octahedral sites; pale blue, Sm (larger) in octahedral sites. The most stable arrangement when the large Sm substitutes for Mg in octahedral sites in trigonal $Mg_3Sb_2$ is for Sm to occupy a majority of octahedral sites in alternate layers in a 2$c$ superstructure, as shown.

system[15] were not realized in the Mg−Sm−Sb system. Rather, this system yields what is, to the best of our knowledge, the first example of a simpler member of the earlier series and not an intergrowth in the true sense. The new compound exemplifies the first superstructure of an $Mg_3Sb_2$-type system, in this case induced by an ordered substitution of the larger dipositive rare-earth element Sm for Mg.

The changes in the $Mg_3Sb_2$ structure type on Sm substitution are illustrated in Figure 1 in ~[110] projections. The parent structure[20] on the left contains hcp slabs of $Mg_2Sb_2$ (dark blue) in which all tetrahedral cavities are filled by Mg (blue). The last third of the Mg (light blue) then occupies all of the nominally octahedral cavities between these four-layer slabs. On addition of some Sm, the refined structure for the ternary example $Mg_{5.231(8)}Sm_{0.769(8)}Sb_4$ on the right, Figure 1, now has 77(1)% of the larger Sm (plus 23% Mg) ordered in one-half of the former interslab layers of octahedral Mg, thereby generating the 2-fold superstructure along $c$ in $P\bar{3}$. (The numbering of the atoms follows the $z$ coordinates, Table 2.) The observed difference in average Mg−Sb distances for the two types of Mg environments (about Mg4 vs Mg2, 3), 0.27 Å, is somewhat larger than that according to standard cation crystal radii for Mg[21] (and a fixed value for $Sb^{3-}$), 0.15 Å, which is some measure of the strain or accommodation in this arrangement. This particular composition, $Mg_{5.231(8)}Sm_{0.769(8)}Sb_4$, was obtained in only 30% yield from the first synthetic success, in which the composition $Mg_5SmSb_4$ had been heated in Ta at 850 °C for 7 days and then cooled. Better and cleaner yields, up

(20) Zintl, E.; Husemann, E. *Z. Phys. Chem.* **1933**, *21B*, 138.
(21) Shannon, R. D. *Acta Crystallogr.* **1976**, *32A*, 751.

to 85%, were obtained after further explorations in which an initial reaction at high temperature was followed either by slow cooling or, best, by annealing the quenched product around 700 °C (see Experimental Section). The sequence is probably necessary because the product melts incongruently. At the same time, an increase of the lattice volume of up to 17.3 Å$^3$ (0.62%) above that for the single-crystal result was observed from a reaction composition $Mg_4Sm_2Sb_4$ quenched from 950 °C and annealed for some time at 700 °C. Obviously, this increase must arise from an increase in Sm content on the substituted sites, which may approach the full limit $Mg_5SmSb_4$, but not to completion in this case inasmuch as SmSb was the other product (more details are given in the Experimental Section).

Furthermore, products from the same series of reactions without excess Sm also exhibited a shifted subcell pattern of a second solution phase $Mg_{3-y}Sm_ySb_2$, evidently reflecting a uniform substitution of Sm on all octahedral sites in the parent structure after the supercell phase approached saturation. The same shifted patterns were also seen in the absence of superstructure phase in earlier reactions that were evidently not at equilibrium. The largest increase seen in the subcell amounted to only 2.2 Å$^3$ ($a \approx 4.586$ Å, $c \approx 7.29$ Å) or 1.93% under the conditions explored, but higher values should be possible. (Substitutions of Yb in the same parent structure were also observed (along with $Yb_{11}Sb_{10}$), but compositions necessary to examine the superstructure formation (or not) were not loaded.) The characteristics of the Sm-substituted phase with the smaller lattice were not studied further. However, its relative stability appears to be appreciably less than that of the superstructure solution inasmuch as substitutions appeared in the smaller cell only after the new ordered phase was close to its Sm limit. Likewise, Sm distributions at intermediate compositions were seen to favor of the larger cell inasmuch as this phase was also richer in Sm than the proportion loaded. It is reasonable that the superstructure should be better able to accommodate the difference in cation radii (below) than a mixture on the unaltered octahedral sites of the parent.

More or less complete substitution in all octahedra are known in $Mg_2AeSb_2$ and related pnictides for Ae = Ca−Ba,[13] but results with less Ae were not noted. In the extreme case, the $Ba^{2+}$ radius is even larger than that of $Sm^{2+}$; however, it's not clear from the isotropic $U$ values reported and the lack of synthetic details whether mixed occupancies of the octahedral sites with some Mg can be excluded, particularly because Ca and Sr refined with smaller values of $U_{iso}$ than did Mg or Sb. Products of a composition that would correspond to that of the ordered supercell, $\sim Mg_5AeSb_4$, have evidently not been investigated for these systems.

Returning to the superstructure phase, the parameters reflect the large difference in standard six-coordinate crystal radii[21] for these two elements, 0.45 or 0.35 Å with 23% Mg mixing; yet the experimental difference in radii within the two types of octahedral sites is in fact only 0.16 Å. Other dimensional changes on formation of the ternary structure do not suggest much further strain or compromises. The small increase in $a$ accompanying the compositional change, 0.06 Å, is reflected in small $< \sim 2°$ flattening of the Sb−Mg−Sb angles about both Mg types to Sb atoms in the same layer, that is, angles that have a component in $c$, but not so for those in the other direction. Likewise, Mg−Sb distances in the common part of the two structures show changes of $\leq 0.02$ Å. On the other hand, although those angles in the octahedra around Mg in the parent structure that have a $c$ component are increased beyond 90° by ~5°, these angles decrease (narrow) by ~6° on Sm substitution. This remains the largest overall change accompanying the substitution, corresponding to a simple expansion of 0.42 Å along $c$ beyond a doubling of that axis. However, a double-sized and fairly uniform displacement ellipsoid for Mg4 in the remaining layered octahedra ($\sim 40 \times 10^3$ Å$^2$, Table 2) suggests some softness or fluxionality in this region.

There is little doubt that alternate substitution of $Eu^{2+}$ or, particularly, the smaller $Yb^{2+}$ should be possible in the new structure, and perhaps other dipositive examples as well. These indeed may further open up rich possibilities for more tuning of properties important to thermoelectric effects, etc. in this structure type. Presumably all of these compounds with only dipositive cations are Zintl phases and semiconductors since creation of cation vacancies would be expected to be energetically unfavorable.

**Acknowledgment.** The principal part of this research was supported by the NSF, Solid State Chemistry, via Grants No. DMR-0129785 and DMR-0444657 and was carried out in the facilities of the Ames Laboratory, U. S. Department of Energy, Iowa State University. The authors also thank the Department of Science and Technology, Government of India and IIT Delhi for the funding of the Bruker SMART APEX X-ray diffractometer.

**Supporting Information Available:** Tables of detailed structural and refinement data and the cif file. This material is available free of charge via the Internet at http://pubs.acs.org.

IC060835W